Mousavi et al., *BioImpacts.* 2026;16:31216
doi:10.34172/bi.31216
https://bi.tbzmed.ac.ir/

# Identifying a *CATSPERB* Variants in unexplained male infertility through familial exome sequencing

**Seyedeh Zahra Mousavi[1], Pegah Kouhi[2], Vahid Esmaeili[3], Zeynab Rokhsattalab[2], Abdolreza Esmaeilzadeh[4], Navid Almadani[2], Bahram Mohammad Soltani[1*], Mehdi Totonchi[2*]**

[1]Department of Molecular Genetics, Faculty of Biological Sciences, Tarbiat Modares University, Tehran, Iran
[2]Department of Genetics, Reproductive Biomedicine Research Center, Royan Institute for Reproductive Biomedicine, ACECR, Tehran, Iran
[3]Department of Embryology, Reproductive Biomedicine Research Center, Royan Institute for Reproductive Biomedicine, ACECR, Tehran, Iran
[4]Department of Immunology, Zanjan University of Medical Sciences, Zanjan, Iran

**Article Info**

***Article Type:***
Original Article

***Article History:***
Received: 5 Apr. 2025
Revised: 16 May 2026
Accepted: 31 May 2026
ePublished: 23 Aug. 2026

***Keywords:***
Unexplained male infertilit
CATSPERB
Missense variation
R709Q alteration
Hyper activation
Familial exome sequencing

**Abstract**

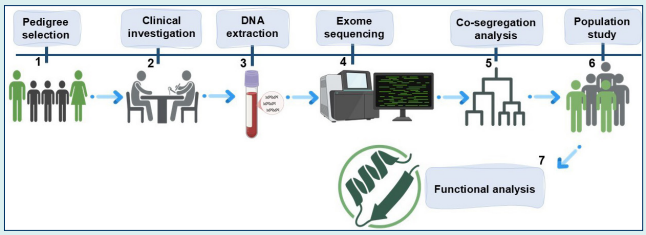


***Introduction:*** Unexplained male infertility (UMI) refers to a situation where no underlying cause of male infertility is defined during investigations of the couple.

***Methods:*** Whole exome sequencing (WES) was performed to identify variants associated with UMI in a consanguineous Iranian family.

***Results:*** WES revealed a rare homozygous missense variant (chr14:g.92088086C>T; NM_024764.4:c.2126G>A; p.Arg709Gln) located in the extracellular region of CATSPERB in three affected siblings. This mutation resulted in the substitution of arginine 709 (R) with glutamine (Q) and co-segregated with the phenotype in other available family members. The kinematic parameters of sperm motility indicated abnormal hyperactivated movement. In-silico protein stability analysis suggests that the Arg709Gln (R709Q) alteration reduces the stability of the CATSPERB protein, potentially compromising causing defects in the overall stability of the CatSper complex.

***Conclusion:*** Our findings provide initial evidence supporting the involvement of *CATSPERB* variants in UMI. This is the first reported genetic variant within the *CATSPERB* gene associated with UMI.

## Introduction

Clinical infertility is defined as the inability of a couple to achieve pregnancy after 12 months of regular, unprotected intercourse.[1] Male-related factors contribute to approximately 50% of infertility cases.[2] The initial step in the laboratory evaluation of male infertility is a conventional semen analysis, which assesses key sperm characteristics including motility, morphology, and viability. Abnormal semen parameters are often indicative of male subfertility.[3] However, approximately 40% of men with infertility have normal semen parameters and receive a diagnosis of unexplained male infertility (UMI), as the underlying cause of infertility remains unknown.[4] UMI is essentially a diagnosis of exclusion, meaning that conventional male factors, including sperm parameters, medical histories, and physical examinations, are normal, with no identifiable reasons found during investigation of the couple.[5-7]

After production, spermatozoa must undergo several processes such as capacitation, zona pellucida binding, surface protein modifications, and chromatin decondensation to successfully traverse the cervical mucus, uterus, and ampullae of the oviducts. Defects in any of these complex events can lead to male infertility.[8] When sperm are exposed to high levels of bicarbonate in the female reproductive tract, it triggers

*Corresponding authors: Bahram Mohammad Soltani, Email: soltanib@modares.ac.ir; Mehdi Totonchi, Email: totonchimehdi@gmail.com

**Research Highlights**

**What is the current knowledge?**

- The CatSper channel is essential for sperm hyperactivation and male fertility.
- Mutations in *CATSPER1* and *CATSPER2* are linked to male infertility.
- The *CATSPERB* variant's role in human male infertility has not been previously reported.

**What is new here?**

- Identification of a rare *CATSPERB* variant (chr14:g.92088086C>T; NM_024764.4:c.2126G>A; p.R709Q) linked to UMI.
- First clinical evidence implicating *CATSPERB* variants in human sperm hyperactivation defects.
- Findings highlight *CATSPERB* as a novel genetic factor for infertility diagnostics.

the activation of soluble adenylate cyclase, resulting in the production of cyclic adenosine monophosphate (cAMP) and the activation of protein kinase A (PKA). PKA induces membrane hyperpolarization through the phosphorylation of tyrosine residues, subsequently activating various calcium channels that enable sperm to acquire hyperactive motility, a significant indicator of sperm capacitation and an absolute requirement for successful fertilization. Hyperactivated sperm are characterized by whip-like, asymmetrical tail bending with high amplitude which relies on an elevation in calcium concentration within the sperm cells.[9,10] Spermatozoa contain various types of Ca2+-permeable channel proteins, including voltage-gated $Ca^{2+}$ (CaV), cyclic nucleotide-gated (CNG), transient receptor potential (TRP), and CatSper channels.[11] As the principal calcium ion channel of sperm, CatSper is sperm-specific and the main gate through which extracellular calcium enters the sperm flagellum, which is essential for fertility.[9,12] The heterotetrameric CatSper complex consists of four distinct pore-forming α subunits (CATSPER1-4) and five documented auxiliary subunits (CATSPERβ, γ, δ, ε, and ζ). CATSPERβ is the first auxiliary protein identified for to the CatSper channel. Using a transgenic approach, CATSPER1 was purified from mouse testis and found to contain the CATSPERβ subunit.[13] Like the CatSper ion channel principal subunits, CATSPERβ was restricted to the testis and localized to the principal piece of the sperm tail. The CATSPERβ protein is absent in CATSPER1−/− sperm, suggesting that it is required for trafficking or formation of a stable channel complex.[10] Disruption of CATSPER genes in mice leads to a lack of CatSper Ca2+ current and a reduction in sperm hyperactivation, while spermatogenesis remains largely unaffected.[13] Genetic mutations can also occur in UMI cases.[14] The clinical diagnosis of these channel abnormalities is crucial for advancing scientific understanding of the significance of the CatSper complex in human sperm.[13]

Previous reports have identified male infertility cases associated with defects in CATSPER1, CATSPER2, and CATSPER3.[12,15,16] To our knowledge, no previous case reports have identified genetic abnormalities in the *CATSPERB* gene among infertile men suffering from UMI. This study presents a unique finding of a rare homozygous missense variant (chr14:g.92088086C>T; NM_024764.4:c.2126G>A; p.R709Q) in the *CATSPERB* gene, identified through whole-exome sequencing (WES) in a consanguineous Iranian family with three affected siblings diagnosed with UMI.

## Materials and Methods

### *Subjects and clinical investigation*

A 36-year-old man was referred to the Infertility and Reproductive Biomedicine Research Center of Royan Institute, Tehran, Iran. During genetic consulting, it was determined that the proband's parents were first cousins and two of his brothers also had infertility. A karyotype analysis was performed on the proband using peripheral blood samples. Informed consent forms were authorized by the Institutional Review Board of Royan Institute Research Center and Royan Ethics Committee in Tehran, Iran, and signed by each participant (IR.ACECR.ROYAN.REC.1396.13). In accordance with the World Health Organization (WHO, 2021) guidelines, two thorough semen analyses were performed for the affected individuals. Since standard clinical investigations failed to identify the cause of the patient's infertility, the family was selected for the study. Both the proband (IV-1) and his brothers (IV-4 and IV-6) and their spouses underwent intracytoplasmic sperm injection (ICSI) to treat their infertility.

### *Study of the sperm parameters*

To ensure there were no issues with morphology, protamination, and acrosome integrity of the sperm, the following tests were performed in addition to routine semen analysis for the individual IV-6.

### *Assessment of the sperm morphology*

Sperm morphology was assessed using the Papanicolaou staining method according to the WHO instructions.[17] First, the smear was prepared according to the protocol and stained using the Papanicolaou method. Then, the morphology of 200 spermatozoa was examined under a 1000× oil-immersion lens using phase-contrast microscopy. Abnormal morphology was assessed in five randomly selected fields of view, and the percentage of abnormal morphology was recorded for each field.

### *Sperm protamine deficiency test by chromomycin A3*

Chromomycin A3 (CMA3) staining was used to assess protamine deficiency. Semen samples were washed twice in $Ca^{2+}$ and $Mg^{2+}$-free phosphate-buffered saline (PBS, pH 7.4). A 50 µL sperm sample was fixed with 50 µL of Carnoy's fixative solution (methanol/glacial acetic acid, 3:1) at 4 °C for 5 minutes. A thin smear of the specimen was prepared and air-dried at room temperature for 30 minutes. The slide was treated with 100 µL of CMA3 solution (Sigma-

Aldrich Co., LLC, St. Louis, MO) for 20 minutes (0.25 mg/mL in 0.15 M PBS, pH 7.4, containing 10 mM MgCl2). Microscopic analysis was performed using a fluorescent microscope with appropriate filters (excitation: 460–495 nm, emission: 510 nm). CMA3 staining was assessed by distinguishing between spermatozoa that stained bright yellow-green (CMA3-positive, deficient in protamine) and those with dull yellow-green staining (CMA3-negative, complete protamine). The percentage of bright yellow-green fluorescent sperm was calculated.

### *Acrosome integrity assessment by PSA–FITC staining*

Acrosome integrity was assessed using fluorescein-conjugated lectin Pisum sativum agglutinin (FITC-PSA).[17] Semen samples were washed twice in $Ca^{2+}$ and $Mg^{2+}$-free PBS (pH = 7.4). The specimens were smeared on the microscope slide, dried, and fixed in 95% ethanol. The smears were stained with FITC-PSA (20 µg/mL) and incubated at 4 ˚C in the dark for 60 minutes. The cells were evaluated using fluorescence microscopy at 1000 × magnification at (excitation: 495–515 nm). Acrosome integrity was assessed by distinguishing between spermatozoa that stained bright green (intact acrosome) and those that did not stain the acrosomal regions (reacted acrosome). The percentage of sperm with bright yellow fluorescence was calculated for each slide.

### *WES and bioinformatics analysis*

Genomic DNA was extracted from peripheral blood samples of the studied family members (III-1, III-2, IV-1, IV-4, and IV-6) using the salting out method. DNA integrity and purity were assessed through gel electrophoresis and NanoDrop (Thermo Fisher Scientific, USA), respectively. Individuals III-1, III-2, IV-1 and IV-4 were selected for WES. The Agilent SureSelect Human All Exon V5 library preparation kit (Agilent, USA) was employed for exome capture. Paired-end reads of 150 base pairs were generated using the Illumina HiSeq 2500 platform and sequenced on lanes of a HiSeq 2500 flow cell. The resulting BCL files were converted to FASTQ format using the built-in Illumina bcl2fastq2 software. Quality control was performed on the FASTQ files using FastQC, followed by trimming using Trimmomatic.[18] The trimmed FASTQ files were then mapped to the UCSC reference human genome assembly GRCh37 (hg19) using the Burrows–Wheeler Aligner (BWA) package version 0.7.17-r1188, generating a SAM file.[19] The SAM format files were converted to BAM format and sorted using SAMtools version 0.1.18.[20] PCR duplicates were marked using Picard tools version 1.107. GATK 4.1.1.1 was utilized for additional processing steps such as base quality recalibration.[21] Variant calling was conducted using HaplotypeCaller.[22] The resulting multi-individual VCF file was annotated using ANNOVAR.[23] A filtration strategy was applied to the annotated variants following the guidelines of the American College of Medical Genetics and Genomics (ACMG).[24] Finally, the shortlisted candidate variants were visualized using IGV 2.5.[25]

### *Co-segregation and sporadic screening of the candidate variant by Sanger sequencing*

The oligonucleotide primers flanking the candidate variant were designed using PerlPrimer software: the forward primer sequence was 5′-CCAAGTCTCTTCTGTTTAATCTCC-3′, and the reverse primer sequence was 5′-GAACCAAGGATAAAGTCAGTCAG-3′.[26] Polymerase chain reaction (PCR) was performed to amplify the target DNA region in the available family members (II-2, III-1, IV-1, IV-4, and IV-6) using the designed primers and Taq DNA polymerase Master Mix (Ampliqon, Odense, Denmark). Sanger sequencing of the amplicons was performed by Macrogen (Seoul, Korea). The sequencing chromatograms were analyzed using CodonCode Aligner v. 5.1.5 software.[27] Additionally, the *CATSPERB* mutation was studied in 39 Iranian men with UMI by Sanger sequencing.

### *Sperm hyperactivation test*

Sperm motility parameters were evaluated using the HFTCASA Computer Aided Semen Analysis System (Hooshmand Fanavar Tehran, Co., Ltd.). The sperm suspension (10 µL) was placed on a slide using a 22 × 22 $mm^2$ coverslip (preparation depth of 20 µm), and the temperature was maintained at 37 °C using a temperature-controlled stage. At least five microscopic fields and a minimum of 300 sperm were analyzed. The following parameters were assessed: curvilinear velocity (VCL, µm/s), straight-line velocity (VSL, µm/s), the amplitude of lateral head displacement (ALH, µm, measuring the magnitude of the lateral displacement of the sperm head about the average path), path velocity (VAP, µm/s), angular displacement (MAD, D), wobble: VAP/VCL (WOB, %), straightness (STR, %), and beat cross frequency (BCF, Hz). Sperm were considered hyperactivated when presenting VCL ≥ 150 µm/s, LIN < 50% and ALH ≥ 3.5 µm.[28]

### *Conservation study and structural in silico modelling*

The evolutionary conservation profile of the CATSPERB protein was analyzed using the Clustal Omega and ConSurf databases.[29,30] As the crystal structure of CATSPERB is not available in the Protein Data Bank (PDB), its predicted 3D structure was obtained from the AlphaFold protein structure database, a revolutionary AI system developed by DeepMind that predicts protein structures from amino acid sequences with unprecedented accuracy.[31] The overall stereochemical quality of each residue in the obtained model was assessed using PROCHECK, which analyzed the Ramachandran plot to evaluate the protein's structural integrity.[32] The generated model was further validated using the ERRAT server, a tool that assesses protein structure quality by analyzing non-bonded atomic interactions and identifying regions that may require refinement. This step ensured the selection of the most reliable structure. Model optimization was

performed using Chimera 1.16 software, and molecular energy minimization was conducted using the YASARA energy minimization server.[33,34] The 3D structures were visualized and analyzed using the PremPS database.[35]

### *Protein stability prediction*

Changes in the stability of the CATSPERB protein due to the R709Q variant were evaluated by MUpro, I-Mutant, and PremPS prediction tools. The results from all servers were reported as ΔΔG values. In most cases, a negative ΔΔG indicates that a single point mutation is destabilizing; however, for PremPS, a positive ΔΔG denotes a destabilizing mutation.[36-38] Additionally, the PremPS tool was used to calculate and visualize the non-covalent interactions between residue number 709 with other residues in the native and mutant CATSPERB protein.

### *Protein-protein interaction (PPI) network construction and pathway enrichment analyses*

Pathway enrichment analyses using the Metascape database were conducted to identify the biological mechanisms associated with the *CATSPERB* gene. The CATSPERB protein was then analyzed using the STRING database (https://string-db.org/) to construct a protein–protein interaction (PPI) network. The PPI network was then visualized using Cytoscape (3.10.2).

### *Accession*

Thevariant(chr14:g.92088086C>T;NM_024764.4:c.2126G>A; p.Arg709Gln) was submitted to ClinVar under accession number SCV004176793 for UMI.

## Results

### *Clinical findings*

The affected siblings (IV-1, IV-4, and IV-6) in the pedigree were the result of a consanguineous marriage, and all had primary infertility (Fig. 1A). Their medical histories and physical examinations showed no notable abnormalities. The proband's karyotype was normal (Table 1). The spouses of the affected did not show any notable infertility-related criteria. Following semen analyses, both the proband (IV-1) and the siblings (IV-4 and IV-6) were diagnosed with UMI (Table 2). Fortunately, the

**Table 1.** Clinical investigations and medical history for three patients with UMI

| Clinical investigations | Patients | | |
|---|---|---|---|
| | IV-1 (Proband) | IV-4 | IV-6 |
| Age(y) | 36 | 30 | 26 |
| History of infertility (y) | 15 | 7 | 2 |
| Cigarette | NO | NO | NO |
| Alcohol | NO | NO | NO |
| Addiction | NO | NO | NO |
| Varicocele | NO | NO | NO |
| Hydrocele | NO | NO | NO |
| Hernia | NO | NO | NO |
| Cryptorchidism | NO | NO | NO |
| Vasectomy | NO | NO | NO |
| Vasoepididymostomy | NO | NO | NO |
| Orchiectomy | NO | NO | NO |
| Allergy | NO | NO | NO |
| Testes size (cm) | 3.5 x 3 | 3.5 x 4 | 3.5 x 3 |
| Testes volume (cc) | 22 | 23 | 22 |
| Testes shape | Normal | Normal | Normal |
| Vas deferens | Normal | Normal | Normal |
| Epididymis | Normal | Normal | Normal |
| Karyotype | Proband: 46, XY<br>Spouse: 46, XX | -<br>- | -<br>- |

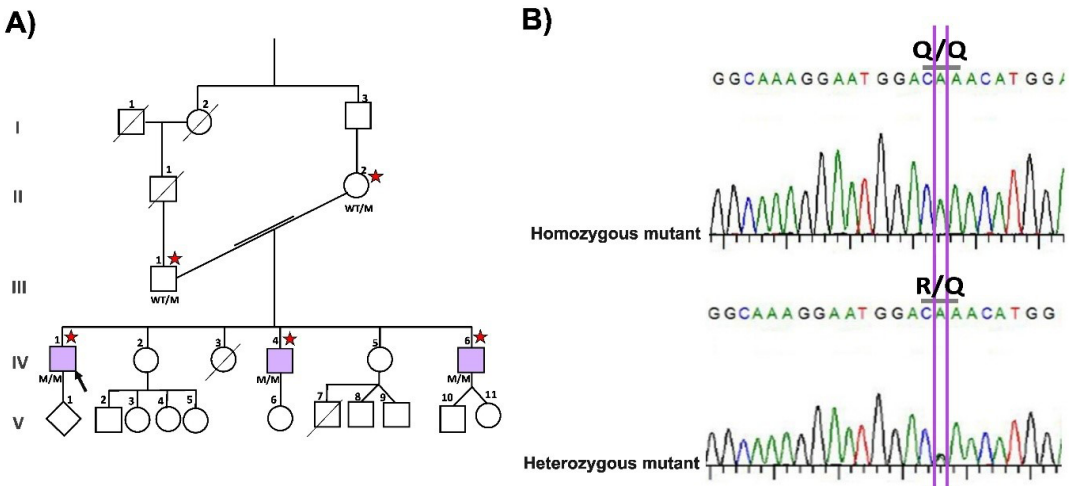


**Fig. 1. (A)** The pedigree of a consanguineous family with UMI and the identified variant. Affected individuals are represented by purple squares, and the proband is indicated by a black arrow. DNA samples from the individuals (II-2, III-1, IV-1, IV-4, and IV-6) were collected (shown by red asterisk signs). Individuals (II-2, III-1, IV-1, and IV-4) were selected for performing exome sequencing, and segregation analysis was performed on (II-2, III-1, IV-1, IV-4, and IV-6) that are shown by red asterisk signs. Sanger sequencing validation results of the intended variant are shown by "WT" for the wild-type allele and "M" for the mutant allele. **(B)** An example of Sanger sequencing confirming the segregation of the *CATSPERB* variant with the phenotype in individuals III-1 (heterozygous) and IV-6 (homozygous). The variant position (c.G2126A) highlighted in a rectangle changes the arginine 709 (R) residue into glutamine (Q).

**Table 2.** Analysis of semen in three patients with UMI

| Semen analysis | | IV-1 (Proband) | IV-4 | IV-6 | Normal range (WHO, 2021) |
|---|---|---|---|---|---|
| | | **Macroscopic evaluation** | | | |
| Semen parameters | Viscosity | Normal | Normal | Normal | Normal |
| | pH | 7.8 | 7.8 | 8 | 7.2 -8.0 |
| | Volume | 7.2 | 4 | 4 | 1.5–7 ml |
| | Liquefaction time | 20 | 20 | 20 | 15–30 min |
| | Color | light-yellow | white-gray | white-gray | - |
| | | **Microscopic evaluation** | | | |
| Sperm number | Total sperm counts | 840 | 576 | 276 | 39.0 or more million |
| Sperm motility | Total motility | 56.8 | 79.6 | 67.6 | |
| | Rapid progressive motility | 18.6 | 19.1 | 30.6 | |
| | Progressive motility | 28.9 | 24.8 | 28.7 | |
| | Total progressive | 47.5 | 43.9 | 59.3 | 32 or more % |
| | Non-progressive motility | 9.3 | 35.7 | 8.3 | |
| | Non-motile | 43.2 | 20.4 | 32.4 | 68 or less % |
| Sperm morphology (%) | Normal morphology | 8 | 5 | 7 | 4.0 or more % |
| | Abnormal morphology | 92 | 95 | 93 | 96.0 or less % |
| | Double head | 1 | - | 1 | |
| | Giant head | 3 | 1 | 5 | |
| | Pin head | 5 | 4 | - | |
| | Short tail | - | 8 | 6 | |
| | Coiled tail | 6 | - | 7 | |
| | Cytoplasm (ERC) | 6 | 1 | - | |

ICSI procedure proved successful for all three affected individuals.

### *Study of the sperm parameters*

The results of the Papanicolaou staining test revealed normal morphology of sperm cells (Fig. 2A). The integrity of the acrosome, a crucial structure involved in fertilization, was assessed using the FITC-PSA staining test, which confirmed that about 78% of the acrosomes in the evaluated sperm samples were intact (Fig. 2B). Furthermore, assessment of sperm protamine content using CMA3 staining indicated that about 74% of sperm cells were completely protaminated, suggesting proper DNA packaging within the sperm nuclei (Fig. 2C). Collectively, these findings provide strong evidence that the assessed sperm parameters, including morphology, protamine content, and acrosome integrity, are within normal ranges.

### *Identification of the CATSPERB mutation*

DNA from two affected brothers (IV-1, IV-4) and their parents (III-1, II-2) underwent WES, with an average coverage of 100X. Approximately 95% of the total reads passed the quality filter ($Q \geq 30$). Common variants ($MAF > 0.05$) identified in publicly available databases were excluded. Consequently, A homozygous exonic single-nucleotide variant in the *CATSPERB* gene (chr14:g.92088086C > T; NM_024764.4:c.2126G > A; p.R709Q) was identified in the two affected brothers (IV-1 and IV-4) (Fig. 3). The Franklin platform (https://franklin.genoox.com/) classified this variant as likely pathogenic according to the ACMG guidelines. The candidate variant replaces R709 with Q and is located in the extracellular region of the CATSPERB protein. This variant is rare in public genomic databases such as GnomAD, ExAC, and the 1000 Genomes Project. There is no record for this variant in the Iranome database. The WES results were confirmed by subsequent Sanger sequencing segregation, which demonstrated the homozygous status of the c.G2126A mutation in the three affected brothers (IV-1, IV-4, IV-6) and heterozygous status in the parents (III-1, II-2). Additionally, the *CATSPERB* mutation co-segregated with the disease in healthy family members (Fig. 1B). Amino acid conservation profile study using the Clustal Omega and ConSurf databases revealed that asparagine 709 is a highly conserved residue (Fig. 4).

### *CATSPERB variant screening in a sporadic Iranian cohort*

The *CATSPERB* mutation (c.2126G > A) was studied in 39 Iranian men with UMI who had normal physical examinations and normal karyotype to evaluate whether this mutation can explain the decline in sperm hyperactivation ability in the population or is privet for this family (Fig. S2). No homozygous or heterozygous patients with the *CATSPERB* (c.2126G > A) mutation were found in this group.

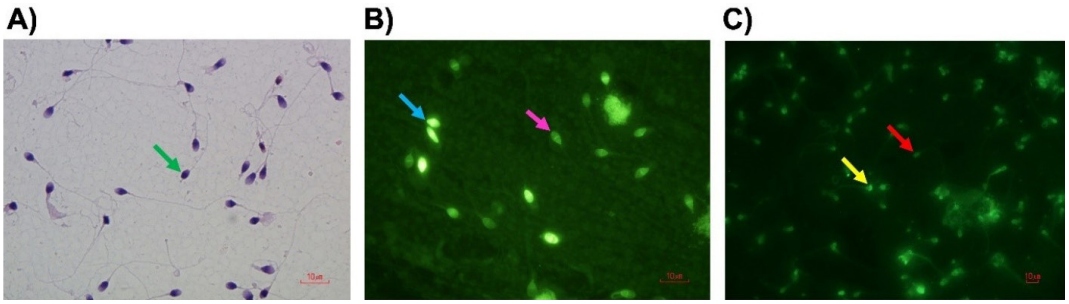


**Fig. 2. Sperm parameter analysis.** (**A**) Sperm morphology test evaluated by Papanicolaou staining (light microscopy, × 10 µm eyepiece magnification). Sperm with normal morphology were observed (green arrow). (**B**) The acrosome integrity was assessed using the FITC-PSA staining. Sperm with intact (purple arrow) and reacted acrosome (blue arrow) were observed. (fluorescent microscopy, × 10 µm eyepiece magnification). (**C**) CMA3 staining of sperm cells to evaluate chromatin protamination. Bright yellow-green stained sperm cells indicate deficient protamination (yellow arrow). Yellowish stained sperm cells show normal protamination content (red arrow) (fluorescent microscopy, × 10 µm eyepiece magnification).

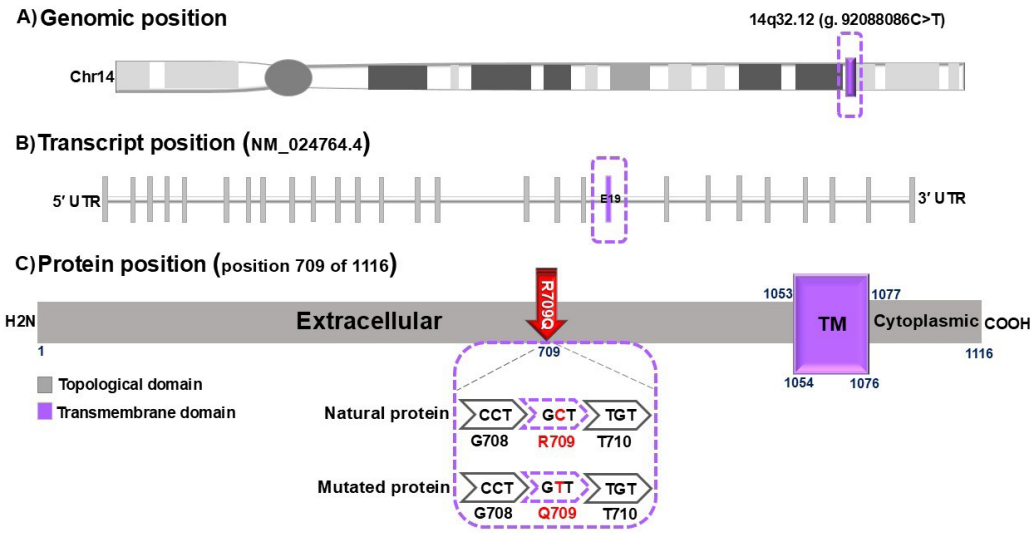


**Fig. 3. The rare CATSPERB variant position. (A)** A schematic representation of the *CATSPERB* genetic map derived from UCSC (hg19) shows its locus on chromosome 14. (**B**) *CATSPERB* transcript exons (E1-E27) are indicated by gray boxes and exon number 19 (E19) is colored purple, while the intronic regions are represented by gray lines. (**C**) The CATSPERB protein has 1116 residues and includes extracellular, transmembrane, and cytoplasmic regions. Our variant occurs in residue 709 in the extracellular domain. The nucleotide sequences of the natural and mutant residues are represented by purple dotted arrows. TM: transmembrane.

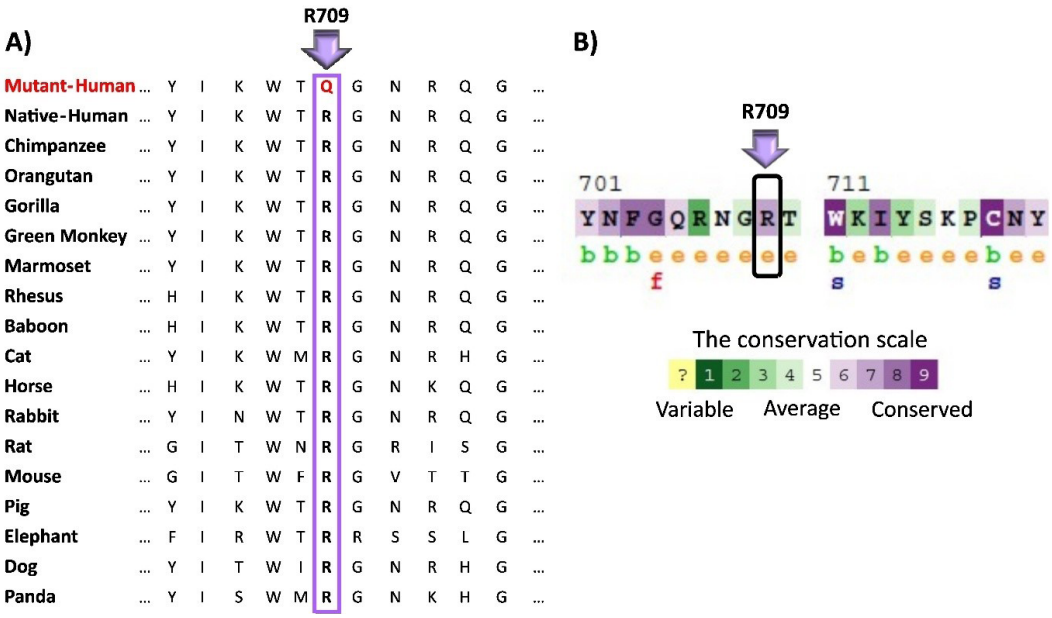


**Fig. 4. CATSPERB conservation study results.** (**A**) Multiple sequence alignments performed using the Clustal Omega server revealed that the R709 residue, indicated by a purple arrow, is highly conserved across eukaryote species. (**B**) The amino acid residues of CATSPERB colored based on conservation scores produced by the ConSurf database.

### *Hyperactivation analysis*

To establish the potential effect of *CATSPERB* mutation in the hyperactivation movement of the sperm that are normal in the fields of motility, count, morphology, acrosome integrity, and chromatin protamination, the Kinematic characteristics of human sperm were evaluated. The results shown in Fig. 5 indicate that this parameter showed that the sperm hyperactivated motility parameters (VCL and ALH) are abnormal.

### *In silico modelling*

The model was constructed by the AlphaFold server; the quality-checking analysis results are as follows: the ERRAT overall quality factor for the model was 90.5039%. The Ramachandran plot from the PROCHECK analysis showed that 90.7%, 8.9%, and 0.3% of the residues were located in the favored, additional allowed, and generously allowed regions, respectively, and only 0.1% were in the disallowed regions (Supplementary file 1, Fig. S1 ). Therefore, the model obtained from the AlphaFold server was reliable and suitable for subsequent analysis.

### *Protein stability and interaction prediction for the CATSPERB mutant*

Three web-based tools, I-Mutant, MUpro, and PremPS, were employed to enhance and refine the accuracy of protein stability prediction. As depicted in Table 3, the ΔΔG values obtained from all prediction tools consistently suggest a decrease in the stability of the mutant protein. Moreover, analysis of the PremPS database on the PDB file obtained from the AlphaFold database revealed the loss of several non-covalent bonds in the mutant CATSPERB protein that were originally present in the wild-type form. Specifically, the missense mutation disrupted a hydrophobic bond with W711, an ionic bond with D532, and polar bonds with D532, G534, F535, and W711, as well as van der Waals bonds with D532, G534, and F535. Interestingly, a new hydrophobic bond formed with residue Q705 in the mutant, but not in the wild-type (Fig. 6). These intricate alterations in the bonding pattern provide valuable insights into the potential functional implications of the mutation within the CATSPERB protein associated with UMI.

**Table 3.** Folding free energy (ΔΔG) and mutant CATSPERB stability situation

| Servers | ΔΔG (kcal/mol) | Stability |
|---|---|---|
| I-Mutant | -1.11 | Stability Decreased |
| Mupro | -1.2788872 | Reduced Stability |
| PremPS | 0.95 | Destabilizing |

### *CATSPERB PPI network construction and pathway enrichment analysis*

The CATSPERB protein name was used to construct a PPI network with the STRING database. The PPI string construction results showed that CATSPER1, CATSPER2, CATSPER3, CATSPER4, CATSPERD, CATSPERE, CATSPERG, CATSPERZ, EFCAB9, and HSPA2 interact with CATSPERB. The Metascape database identifies enriched pathways associated with the *CATSPERB* gene, including sperm motility and taxes, sperm capacitation and spermatogenesis (Fig. 7).

## Discussion

Sperm cells once released into the lumen of the

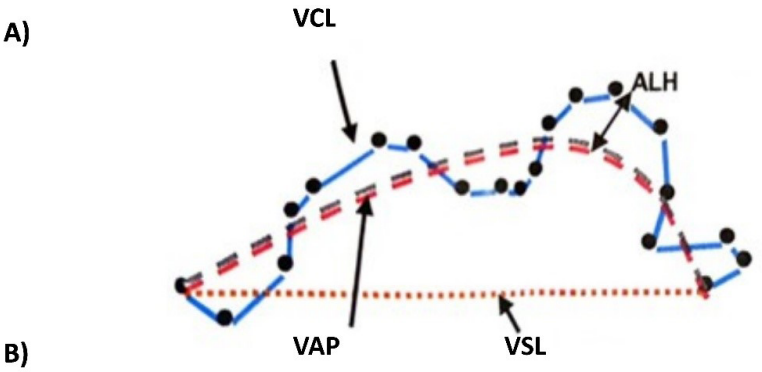


| Sperm dynamic parameters | Definition | Calculated value | Normal range for hyperactivation |
|---|---|---|---|
| VSL (μm/s) | Straight line velocity | 19.99 | ----- |
| VCL (μm/S) | Curvilinear (actual) path velocity | 26.04 | VCL ≥ 150 |
| ALH (μm/S) | Amplitude of lateral head displacement | 0.94 | ALH ≥ 3.5 |
| LIN (%) | Linearity (VSL/VCL) | 43.99 | < 50% |
| VAP (μm/s) | Average path velocity | 22.28 | ----- |
| BCF (Hz) | Beat cross frequency | 3.05 | ----- |
| MAD (D) | Angular displacement | 12.46 | ----- |
| STR (%) | Straighness (VSL/VAP) | 51.67 | ----- |
| WOB (%) | Wobble (VAP/VCL) | 51.67 | ----- |

**Figure 5.** Sperm dynamic parameters related to individual IV-6. (**A**) Schematic representation of sperm kinematic characteristics as measured by the HFTCASA Computer Aided Semen Analysis System, illustrating dynamic motility parameters assessed in this study. (**B**) Quantitative kinematic characteristics of spermatozoa from individual IV-6, showing values related to motility parameters.

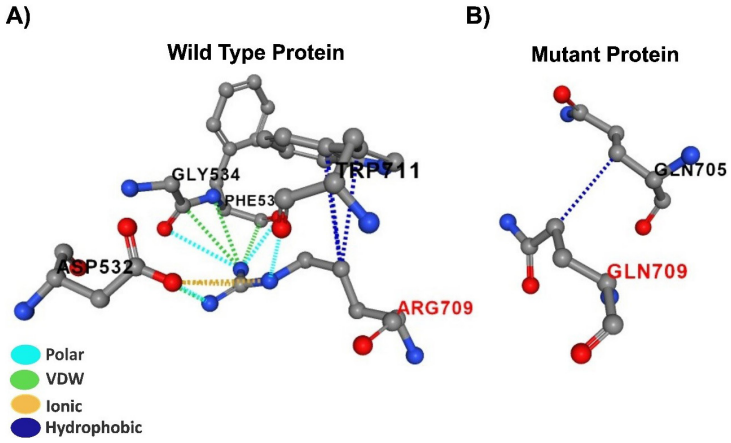


**Fig. 6. (A)** Native (R709) and **(B)** Mutant (R709Q) CATSPERB residues interactions.

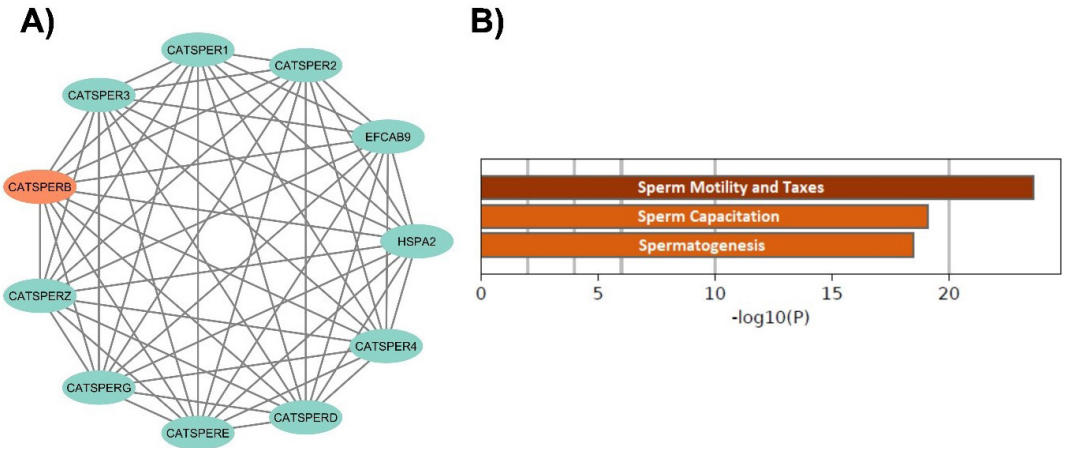


**Fig. 7. PPI Network and Pathways Enrichment**. **(A)** CATSPERB PPI Networks constructed **(B)** Metascape database pathways associated with CATSPERB.

seminiferous tubules are structurally complete but remain functionally immature. During their transit through the epididymis, sperm cells undergo essential maturation processes that are vital for them to acquire their functionalities.[36] $Ca^{2+}$ is crucial for sperm motility, capacitation, the acrosome reaction, sperm-egg fusion, and the induction of the fertilization wave in eggs during mammalian fertilization.[37] The capacitation process includes three $Ca^{2+}$-mediated events: initial activation, hyperactivation of motility, and engagement of a protein kinase cascade. It enables the sperm to fertilize the egg once it reaches the female reproductive tract. Changes in intracellular $Ca^{2+}$, cAMP, and pH levels are necessary for these processes to occur. Male infertility can result from genetic abnormalities that affect any of these processes.[38] During sperm capacitation, the CatSper channel, which is a $Ca^{2+}$-permeant channel, causes sperm hyperactivation and mediates the predominant $Ca^{2+}$-carrying current in mouse epididymal spermatozoa.[11] The CatSper complex is expressed in the testis and is primarily localized to the principal piece of the sperm tail.[10] The extracellular domain of the CATSPERB subunit potentially modulates the channel through external signals such as ligands and cell-cell communication during sperm maturation in the epididymis and/or in the female reproductive tract.[9] Genetic abnormalities can frequently impact spermatogenesis or sperm function, leading to male infertility.[38] In this study, WES identified a rare homozygous exonic variant in the extracellular domain of CATSPERB (chr14:g.92088086C > T; NM_024764.4:c.2126G > A; p.R709Q) in three affected siblings (IV-1, IV-4, IV-6) with UMI in an Iranian family. The variant was successfully validated and co-segregated with the UMI phenotype. Arginine is a larger, positively charged residue, whereas glutamine is smaller and uncharged. The R709Q mutation results in the loss of a positive charge and a smaller side chain, potentially disrupting interactions with other molecules or residues. This assumption is supported by findings from the PremPS database, which provide additional insights into the impact of the R709Q mutation. The mutant residue displayed an altered interaction profile compared to the native residue. The presence of multiple non-covalent interactions, such as polar, van der Waals, ionic, and hydrophobic bonds, in the native residue suggests a more intricate network of molecular associations. These interactions are crucial for stabilizing protein structures and facilitating various biological processes. The disruption of these interactions caused by the R709Q mutation could lead to functional consequences. The mutant residue's interaction profile was limited to a single hydrophobic bond with Q705. This specific interaction, absent in the native residue, indicates

a difference in mode of engagement between the native and mutant forms. These results, based on the potential role of the mouse CATSPERB subunit in protein stability, suggested that the R709Q mutation may significantly impact the overall structure and function of the CatSper complex.[10]

The CatSper complex genes in knock-out mice affect sperm hyperactivation but do not affect sperm production or morphology. This suggests that this complex does not affect spermatogenesis in mice but is important for sperm hyperactivation.[13] Sperm from knocked-out Catsper1 mice are unable to fertilize intact eggs, but fertilization occurs in those oocytes whose outer layers have been enzymatically removed. Furthermore, in WT sperm cells, depolarization induces an increase in intracellular $Ca^{2+}$, whereas it does not in spermatozoa lacking Catsper1. CatSperb is absent in sperm from mice lacking CatSper1, suggesting that the expression of CatSperb and Catsper1 is linked. CatSper-knockout males show poor sperm motility and are sterile. The targeted knock-out of Catsper2, Catsper3, and Catsper4 in mice lacking the hyperactivated motility required for fertilization and their phenotype was the same as that of Catsper1 knock-out animals. Altogether, *CATSPER* genes appear to have similarly essential roles in sperm hyperactivation and fertility.[10,39] Interestingly, the affected individuals in our studied pedigree produced sperm with normal counts and morphology. Furthermore, other sperm parameters, such as DNA condensation and acrosome integrity, were normal. Remarkably, the CASA parameters showed that the sperm problems in the affected individuals under study were associated with hyperactivation. Sperm lacking the CatSper current were unable to respond to CatSper activation by progesterone, resulting in fertilization failure during in vitro fertilization (IVF) procedures.[40] However, despite this challenge, individuals from this pedigree were able to achieve a successful pregnancy by undergoing ICSI procedures. This suggests a potential compensatory role for CatSper in sperm hyperactivation. Exploring the underlying molecular mechanisms behind the absence or reduced functionality of the CatSper channel could provide valuable insights into potential therapeutic interventions. Targeting these mechanisms may offer promising strategies for the treatment of male infertility associated with CatSper channel dysfunction. Despite the novel findings reported in this study, several limitations should be considered. The small sample size and genetic analysis performed on a single family limit the generalizability of these findings to a broader population. Additionally, functional validation experiments to directly confirm the biological impact and molecular function of the *CATSPERB* R709Q variant were not conducted. Future studies involving larger cohorts and comprehensive functional assays are necessary to better understand the pathogenic role of this variant and its contribution to UMI.

## Conclusion

This study reports, for the first time, a mutation in the *CATSPERB* subunit of CatSper associated with UMI. The potential absence of the CatSper $Ca^{2+}$ current due to the R709Q mutation in the CATSPERB subunit in sperm from the affected individuals resulted in failed sperm hyperactivation. However, the individuals achieved successful pregnancies through ICSI. Further research is needed better to understand the implications of CatSper deficiency on male fertility and to explore potential therapeutic approaches.

### Acknowledgements

This work was financially supported in part by grants from the Department of Genetics at Royan Institute for Reproductive Biomedicine, Tehran, Iran, the Headquarters for Development of Regenerative Medicine and Stem Cell Technologies at the Vice Presidency for Science and Technology of the Presidential Administration, Tehran, Iran, and the National Institute for Medical Research Development (NIMAD), Tehran, Iran.

### Authors' Contribution

**Conceptualization:** Seyedeh Zahra Mousavi, Mehdi Totonchi.
**Data curation:** Seyedeh Zahra Mousavi.
**Formal analysis:** Seyedeh Zahra Mousavi, Vahid Esmaeili.
**Funding acquisition:** Mehdi Totonchi.
**Investigation:** Seyedeh Zahra Mousavi, Pegah Kouhi, Navid Almadani, Mehdi Totonchi, Zeynab Rokhsattalab.
**Methodology:** Seyedeh Zahra Mousavi, Mehdi Totonchi.
**Project administration:** Mehdi Totonchi.
**Resources:** Seyedeh Zahra Mousavi, Abdolreza Esmaeilzadeh, Mehdi Totonchi.
**Supervision:** Mehdi Totonchi, Bahram Mohammad Soltani.
**Validation:** Seyedeh Zahra Mousavi, Pegah Kouhi.
**Visualization:** Seyedeh Zahra Mousavi.
**Writing–original draft:** Seyedeh Zahra Mousavi.
**Writing–review and editing:** Seyedeh Zahra Mousavi, Mehdi Totonchi.

### Competing Interests

The authors declare that they have no known competing financial or non-financial interests that could have influenced the work reported in this paper.

### Data Availability Statement

WES data sharing is not applicable.

### Declaration of AI-Assisted Tools in the Writing Procedure

The authors declare that AI-assisted technology (Perplexity) was used during the grammar editing process of this manuscript. The use of AI tools did not influence the scientific content or data analysis.

### Ethical Approval

The authors declare that this study was conducted in accordance with the ethical standards of the Institutional Review Board of Royan Institute Research Center and Royan Ethics Committee in Tehran, Iran (IR.ACECR.ROYAN.REC.1396.13). Informed consent was obtained from all participants involved in the study.

### Funding

This research was supported by the Royan Institute for Reproductive Biomedicine, Tehran, Iran.

### Supplementary files

Supplementary file 1 contains Figs. S1 and S2.

### References

1. Awonuga AO, Camp OG, Biernat MM, Abu-Soud HM. Overview of infertility. *Syst Biol Reprod Med* **2025**; 71: 116-42. doi:10.1080/19396368.2025.2469582

2. Kusibab K, Sikora G, Woźniak M, Kutnik K, Koguc K, Czechowski M, et al. The effects of cannabis on male fertility: a literature review. *Quality in Sport* **2025**; 45: 66516. doi:10.12775/qs.2025.45.66516
3. Panner Selvam MK, Agarwal A, Pushparaj PN, Baskaran S, Bendou H. Sperm proteome analysis and identification of fertility-associated biomarkers in unexplained male infertility. *Genes (Basel)* **2019**; 10: 522. doi:10.3390/genes10070522
4. Corsini C, Boeri L, Candela L, Pozzi E, Belladelli F, Capogrosso P, et al. Is there a relevant clinical impact in differentiating idiopathic versus unexplained male infertility? *World J Mens Health* **2023**; 41: 354-62. doi:10.5534/wjmh.220069
5. Jaiswal A, Baliu-Souza T, Turner K, Nadiminty N, Rambhatla A, Agarwal A, et al. Sperm centriole assessment identifies male factor infertility in couples with unexplained infertility - a pilot study. *Eur J Cell Biol* **2022**; 101: 151243. doi:10.1016/j.ejcb.2022.151243
6. Abdallah KS, Hunt S, Abdullah SA, Mol BW, Youssef MA. How and why to define unexplained infertility? Semin Reprod Med **2020**; 38: 55-60. doi:10.1055/s-0040-1718709
7. Zhang T, Dong F, Zhang X, Ping P, Qiu J, Lu Z, et al. Insights from a Pseudo-Polygyny Cohort unmasking high sperm concentration and low forward motility as potential risk factors for recurrent failure of sperm donation IVF (RFDI), a subset of unexplained male infertility (UMI). *EBioMedicine* **2025**; 119: 105871. doi:10.1016/j.ebiom.2025.105871
8. Banjoko SO, Adeseolu FO. Seminal plasma pH, inorganic phosphate, total and ionized calcium concentrations in the assessment of human spermatozoa function. *J Clin Diagn Res* **2013**; 7: 2483-6. doi:10.7860/jcdr/2013/6194.3585
9. Rahban R, Nef S. CatSper: the complex main gate of calcium entry in mammalian spermatozoa. *Mol Cell Endocrinol* **2020**; 518: 110951. doi:10.1016/j.mce.2020.110951
10. Liu J, Xia J, Cho KH, Clapham DE, Ren D. CatSperβ, a novel transmembrane protein in the CatSper channel complex. *J Biol Chem* **2007**; 282: 18945-52. doi:10.1074/jbc.M701083200
11. Cai X, Clapham DE. Evolutionary genomics reveals lineage-specific gene loss and rapid evolution of a sperm-specific ion channel complex: CatSpers and CatSperβ. *PLoS One* **2008**; 3: e3569. doi:10.1371/journal.pone.0003569
12. Wang J, Tang H, Zou Q, Zheng A, Li H, Yang S, et al. Patient with CATSPER3 mutations-related failure of sperm acrosome reaction with successful pregnancy outcome from intracytoplasmic sperm injection (ICSI). *Mol Genet Genomic Med* **2021**; 9: e1579. doi:10.1002/mgg3.1579
13. Luo T, Chen HY, Zou QX, Wang T, Cheng YM, Wang HF, et al. A novel copy number variation in CATSPER2 causes idiopathic male infertility with normal semen parameters. *Hum Reprod* **2019**; 34: 414-23. doi:10.1093/humrep/dey377
14. Esteves SC. A clinical appraisal of the genetic basis in unexplained male infertility. *J Hum Reprod Sci* **2013**; 6: 176-82. doi:10.4103/0974-1208.121419
15. Avenarius MR, Hildebrand MS, Zhang Y, Meyer NC, Smith LL, Kahrizi K, et al. Human male infertility caused by mutations in the CATSPER1 channel protein. *Am J Hum Genet* **2009**; 84: 505-10. doi:10.1016/j.ajhg.2009.03.004
16. Avidan N, Tamary H, Dgany O, Cattan D, Pariente A, Thulliez M, et al. CATSPER2, a human autosomal nonsyndromic male infertility gene. *Eur J Hum Genet* **2003**; 11: 497-502. doi:10.1038/sj.ejhg.5200991
17. World Health Organization (WHO). *WHO Laboratory Manual for the Examination of Human Semen and Sperm-Cervical Mucus Interaction*. Cambridge University Press; **1999**.
18. Bolger AM, Lohse M, Usadel B. Trimmomatic: a flexible trimmer for Illumina sequence data. *Bioinformatics* **2014**; 30: 2114-20. doi:10.1093/bioinformatics/btu170
19. Li H, Durbin R. Fast and accurate short read alignment with Burrows-Wheeler transform. *Bioinformatics* **2009**; 25: 1754-60. doi:10.1093/bioinformatics/btp324
20. Li H, Handsaker B, Wysoker A, Fennell T, Ruan J, Homer N, et al. The sequence alignment/map format and SAMtools. *Bioinformatics* **2009**; 25: 2078-9. doi:10.1093/bioinformatics/btp352
21. McKenna A, Hanna M, Banks E, Sivachenko A, Cibulskis K, Kernytsky A, et al. The Genome Analysis Toolkit: a MapReduce framework for analyzing next-generation DNA sequencing data. *Genome Res* **2010**; 20: 1297-303. doi:10.1101/gr.107524.110
22. Lefouili M, Nam K. The evaluation of Bcftools mpileup and GATK HaplotypeCaller for variant calling in non-human species. *Sci Rep* **2022**; 12: 11331. doi:10.1038/s41598-022-15563-2
23. Wang K, Li M, Hakonarson H. ANNOVAR: functional annotation of genetic variants from high-throughput sequencing data. *Nucleic Acids Res* **2010**; 38: e164. doi:10.1093/nar/gkq603
24. Green RC, Berg JS, Grody WW, Kalia SS, Korf BR, Martin CL, et al. ACMG recommendations for reporting of incidental findings in clinical exome and genome sequencing. *Genet Med* **2013**; 15: 565-74. doi:10.1038/gim.2013.73
25. Thorvaldsdóttir H, Robinson JT, Mesirov JP. Integrative Genomics Viewer (IGV): high-performance genomics data visualization and exploration. *Brief Bioinform* **2013**; 14: 178-92. doi:10.1093/bib/bbs017
26. Marshall OJ. PerlPrimer: cross-platform, graphical primer design for standard, bisulphite and real-time PCR. *Bioinformatics* **2004**; 20: 2471-2. doi:10.1093/bioinformatics/bth254
27. Richterich P. CodonCode aligner version 1.2 released. *Genet Med* **2004**; 6: 162-3. doi:10.1097/00125817-200405000-00012
28. Mortimer ST, Swan MA, Mortimer D. Effect of seminal plasma on capacitation and hyperactivation in human spermatozoa. *Hum Reprod* **1998**; 13: 2139-46. doi:10.1093/humrep/13.8.2139
29. Sievers F, Higgins DG. Clustal omega. *Curr Protoc Bioinformatics* **2014**; 48: 3-13. doi:10.1002/0471250953.bi0313s48
30. Yariv B, Yariv E, Kessel A, Masrati G, Chorin AB, Martz E, et al. Using evolutionary data to make sense of macromolecules with a "face-lifted" ConSurf. *Protein Sci* **2023**; 32: e4582. doi:10.1002/pro.4582
31. Jumper J, Evans R, Pritzel A, Green T, Figurnov M, Ronneberger O, et al. Highly accurate protein structure prediction with AlphaFold. *Nature* **2021**; 596: 583-9. doi:10.1038/s41586-021-03819-2
32. Laskowski RA, MacArthur MW, Moss DS, Thornton JM. PROCHECK: a program to check the stereochemical quality of protein structures. *J Appl Crystallogr* **1993**; 26: 283-91. doi:10.1107/s0021889892009944
33. Meng EC, Goddard TD, Pettersen EF, Couch GS, Pearson ZJ, Morris JH, et al. UCSF ChimeraX: tools for structure building and analysis. *Protein Sci* **2023**; 32: e4792. doi:10.1002/pro.4792
34. Land H, Humble MS. YASARA: a tool to obtain structural guidance in biocatalytic investigations. *Methods Mol Biol* **2018**; 1685: 43-67. doi:10.1007/978-1-4939-7366-8_4
35. Chen Y, Lu H, Zhang N, Zhu Z, Wang S, Li M. PremPS: Predicting the impact of missense mutations on protein stability. *PLoS Comput Biol* **2020**; 16: e1008543. doi:10.1371/journal.pcbi.1008543
36. Hart HM, Nixon B, Martin JH, Aitken RJ, De Iuliis GN. Improving sperm selection strategies for assisted reproduction through closing the knowledge gap in sperm maturation mechanics. *Hum Reprod Open* **2025**; 2025: hoaf040. doi:10.1093/hropen/hoaf040
37. Allard-Phillips E, Kolli S, Rhoton-Vlasak A, Campbell K. Systematic review of the impact of calcium channel blockers on sperm function. *Reprod Toxicol* **2025**; 132: 108841. doi:10.1016/j.reprotox.2025.108841
38. Hildebrand MS, Avenarius MR, Fellous M, Zhang Y, Meyer NC, Auer J, et al. Genetic male infertility and mutation of CATSPER ion channels. *Eur J Hum Genet* **2010**; 18: 1178-84. doi:10.1038/ejhg.2010.108
39. Patankar A, Gajbhiye R, Surve S, Parte P. Epigenetic landscape of testis specific histone H2B variant and its influence on sperm function. *Clin Epigenetics* **2021**; 13: 101. doi:10.1186/s13148-021-01088-4
40. Williams HL, Mansell S, Alasmari W, Brown SG, Wilson SM, Sutton KA, et al. Specific loss of CatSper function is sufficient to compromise fertilizing capacity of human spermatozoa. *Hum Reprod* **2015**; 30: 2737-46. doi:10.1093/humrep/dev243